Available online at www.sciencedirect.com

SciVerse ScienceDirect

Ceramics International 38 (2012) 1127–1132

CERAMICS INTERNATIONAL

www.elsevier.com/locate/ceramint

Microwave dielectric properties of multi-ions $Ba(Zn,Ta)O_3$-based perovskite ceramics

Sea-Fue Wang *, Yuh-Ruey Wang, Chung-Yu Liu, Wen-Shuo Hsieh

Department of Materials and Mineral Resources Engineering, National Taipei University of Technology, Taipei, Taiwan, ROC

Received 14 July 2011; received in revised form 16 August 2011; accepted 17 August 2011
Available online 26 August 2011

Abstract

In this study, $Ba(Zn_{1/3}Ta_{2/3})O_3$-based complex perovskite compounds, including $Ba(Zn_{1/3}Ta_{2/3})O_3$, $Ba(Zn_{1/3}Ta_{1/3}Nb_{1/3})O_3$, $Ba(Zn_{1/6}Co_{1/6}Ta_{2/9}Nb_{2/9}Sb_{2/9})O_3$, and $Ba_{1/2}Sr_{1/2}(Zn_{1/6}Co_{1/6}Ta_{2/9}Nb_{2/9}Sb_{2/9})O_3$, were prepared and characterized. There was no second phase formation shown in the XRD patterns. Though it has been suggested that substitutions of multiple ions over A-site or B-site of the $Ba(Zn_{1/3}Ta_{2/3})O_3$ ceramics may not be beneficial to their microwave dielectric properties, the $Ba(Zn_{1/6}Co_{1/6}Ta_{2/9}Nb_{2/9}Sb_{2/9})O_3$ and $Ba_{1/2}Sr_{1/2}(Zn_{1/6}Co_{1/6}Ta_{2/9}Nb_{2/9}Sb_{2/9})O_3$ ceramics in this study were found to perform in a fairly acceptable manner. The $Ba(Zn_{1/6}Co_{1/6}Ta_{2/9}Nb_{2/9}Sb_{2/9})O_3$ ceramic (sintered at 1575 °C for 6 h) and the $Ba_{1/2}Sr_{1/2}(Zn_{1/6}Co_{1/6}Ta_{2/9}Nb_{2/9}Sb_{2/9})O_3$ ceramic (sintered at 1550 °C for 6 h) reported the following characteristics after annealing at 1400 °C for 10 h: 24.9 and 27.0 for dielectric constants (ε_r), 83,000 and 32,100 GHz for quality factors ($Q \times f$) values and −12.8 and −22.6 ppm/°C for temperature coefficients of resonance frequency (τ_f).

Keywords: A. Sintering; B. X-ray methods; C. Dielectric properties; Microstructure; Complex perovskite

1. Introduction

The market of commercial wireless communication has witnessed a rapid growth during the past decade thanks to technology advancement made possible, in part, by the recent revolution in the miniaturization of microwave circuits by using high dielectric constant (ε_r), low-loss (high Q), and temperature stable (low τ_f) dielectric resonators. Several ceramic materials, including $(Zr_{0.8}Sn_{0.2})TiO_4$, $Ba(Zn,Ta)O_3$, $BaTi_4O_9$, $Ba_2Ti_9O_{20}$, and $BaO–R_2O_3–TiO_2$ (R = rare earth ions) systems, have been developed for use as microwave resonators [1–6]. Among the various candidates, microwave dielectric ceramics based on the $Ba(Zn_{1/3}Ta_{2/3})O_3$ ceramic, a 1:2 $Ba(B'B'')O_3$-type complex perovskite, in particular have been widely used in the electronics industry because of their high dielectric constants (greater than 25), good quality factors (Q over 3000 at 10 GHz), and low (near-zero) temperature coefficients [4,7,8].

The ordering of complex perovskite $Ba(Zn_{1/3}Ta_{2/3})O_3$ is a subject of interest in the area of microwave communication because the 1/3 ⟨1 1 1⟩ ordering is generally believed to be closely related to the high-Q property of $Ba(Zn_{1/3}Ta_{2/3})O_3$ [9–11]. In the literature, $Ba(Zn_{1/3}Ta_{2/3})O_3$ ceramics were observed to achieve a high Q value after being annealed for an extended time at above 1400 °C, inducing cation ordering on the B site along the κ direction [7,12]. However, it was also reported that the high Q value of $Ba(Zn_{1/3}Ta_{2/3})O_3$ could be attributed to the volatilization of the ZnO after long high-temperature sintering [13]. Ba^{2+} replaced the lost Zn^{2+} on the B sites, causing lattice distortions since the ionic radius of the former is larger than that of the latter. On the other hand, Tamura et al. suggested that the enhancement of the Q value was not related to cation ordering [14]. Davies et al. showed that the high Q value observed in $Ba(Zn_{1/3}Ta_{2/3})O_3–BaZrO_3$ ceramics was related to the stabilization of the grain boundary and the lowing of the free energy of the anti-phase boundaries [15]. Lee et al. reported that the $Q \times f$ value of $Ba(Zn_{1/3}Ta_{2/3})O_3$ ceramic decreased with increasing B_2O_3 content, in spite of the highly ordered 1:2 structure [11].

* Corresponding author. Present address: Department of Materials and Mineral Resources Engineering, National Taipei University of Technology, 1, Sec. 3, Chung-Hsiao E. Rd., Taipei 106, Taiwan, ROC.
Tel.: +886 2 2771 2171x2735; fax: +886 2 2731 7185.
E-mail addresses: sfwang@ntut.edu.tw, seafuewang@yahoo.com (S.-F. Wang).

0272-8842/$36.00
doi:10.1016/j.ceramint.2011.08.040

It has been found that the substitution of Ba^{2+} by Sr^{2+} in $Ba(Zn_{1/3}Ta_{2/3})O_3$ ceramics led to decrease in $Q \times f$ value and variation in τ_f value due to the structural distortion caused by octahedral titling [16]. The slightly more complicated systems of several other groups, including $Ba(Zn_{1/3}Ta_{2/3})O_3$–$(Sr,Ba)(Ga_{1/2}Ta_{1/2})O_3$, $Ba(Co_{1/3}Nb_{2/3})O_3$–$Sr(Zn_{1/3}Nb_{2/3})O_3$, and $Ba(Mg_{1/3}Ta_{2/3})O_3$–$Ba(Co_{1/3}Nb_{2/3})O_3$ ceramics, were explored to improve the microwave dielectric properties of complex perovskites [17,18]. Though little is known about the effect of the multiple ion substitution on the microwave dielectric properties of the complex perovskites in the literature, it is generally believed that the microwave dielectric properties may be degraded by the substitution of multiple ions over the A-site and B-site of the perovskites as a variety of ions may increase structural complexity and blow up the cation-ordering on the B site. In this study, Nb^{5+}, Sb^{5+}, Co^{2+}, and Sr^{2+} ions were used to substitute Ta^{5+} and Zn^{2+} at the B-site and Ba^{2+} at the A-site of the $Ba(Zn_{1/3}Ta_{2/3})O_3$ complex perovskite. In additional to the $Ba(Zn_{1/3}Ta_{2/3})O_3$ ceramic, $Ba(Zn_{1/3}Ta_{1/3}Nb_{1/3})O_3$, $Ba(Zn_{1/6}Co_{1/6}Ta_{2/9}Nb_{2/9}Sb_{2/9})O_3$, and $Ba_{1/2}Sr_{1/2}(Zn_{1/6}Co_{1/6}Ta_{2/9}Nb_{2/9}Sb_{2/9})O_3$ ceramics were prepared. Their densification, microstructural evolution, and microwave dielectric properties were characterized and discussed.

2. Experimental procedure

Pre-calcined powders of perovskite ceramics were prepared using the solid-state reaction technique. High-purity (>99.9% purity) TiO_2, $BaCO_3$, ZnO, Ta_2O_5, $CoCO_3$, Sb_2O_5, and Nb_2O_5 (all STREM Chemicals, Reagent grade) were used as raw materials. Oxides based on the compositions of $Ba(Zn_{1/3}Ta_{2/3})O_3$, $Ba(Zn_{1/3}Ta_{1/3}Nb_{1/3})O_3$, $Ba(Zn_{1/6}Co_{1/6}Ta_{2/9}Nb_{2/9}Sb_{2/9})O_3$, and $Ba_{1/2}Sr_{1/2}(Zn_{1/6}Co_{1/6}Ta_{2/9}Nb_{2/9}Sb_{2/9})O_3$, as listed in Table 1 were mixed and milled in methyl alcohol solution using polyethylene jars and zirconia balls for 24 h and then dried at 80 °C in an oven overnight. After drying, the powders were calcined at the temperatures ranging from 1100 °C to 1300 °C for 2 h, and then re-milled in methyl alcohol for 24 h. Phase identification on the calcined powders was performed using X-ray diffraction (XRD, Simens D5000). The powder was added with a 5 wt% of 15%-PVA solution and pressed into disc-shaped compacts under a uniaxial pressure of 0.9 tons/cm^2. The samples were then heat treated at 550 °C for 4 h to eliminate the PVA, followed by sintering at 1525 °C, 1550 °C, 1575 °C, 1600 °C, 1625 °C, and 1650 °C for 6 h (heating rate = 10 °C/min). Selected samples were then annealed at 1400 °C for 10 and 24 h.

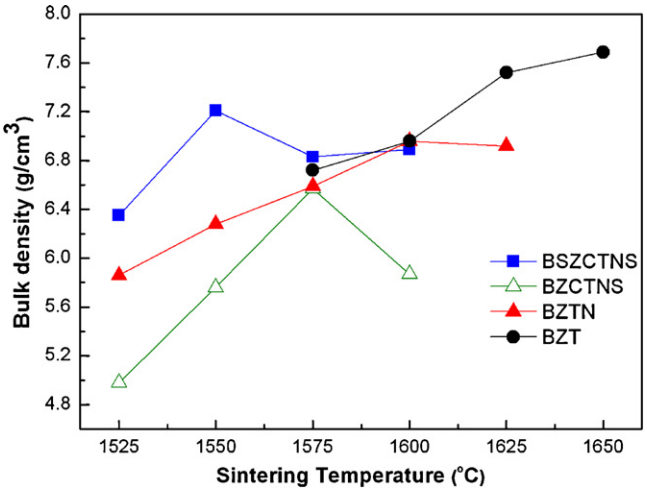

Fig. 1. Sintered densities versus sintering temperatures for the $Ba(Zn_{1/3}Ta_{2/3})O_3$, $Ba(Zn_{1/3}Ta_{1/3}Nb_{1/3})O_3$, $Ba(Zn_{1/6}Co_{1/6}Ta_{2/9}Nb_{2/9}Sb_{2/9})O_3$, and $Ba_{1/2}Sr_{1/2}(Zn_{1/6}Co_{1/6}Ta_{2/9}Nb_{2/9}Sb_{2/9})O_3$ ceramics.

Densities of the specimens were measured using the liquid displacement method. Phase identification of the sintered bulk ceramics was conducted using XRD. The microstructures of the sintered samples were observed by scanning electron microscopy (SEM, JEOL 6500F) with an energy-dispersive spectroscopy (EDS). The samples used for SEM observation were thermally etched at 1480 °C for 12 min. The densified cylindrical samples were polished to have an exact thickness of 5 mm for measuring microwave properties. The dielectric constants and unloaded Q values at microwave frequencies were measured in the $TE_{0\,1\,\delta}$ mode using the Hakki and Colleman method [19] and a network analyzer (HP 8722ES). Measurements of the temperature coefficient of the resonant frequency τ_f in the temperature range from 25 to 85 °C were performed in a Delta Design box furnace. The τ_f was defined by $(f_T - f_{25})/f_{25}(T - 25\ ^\circ C)$.

3. Results and discussion

Fig. 1 presents the sintered densities of the $Ba(Zn_{1/3}Ta_{2/3})O_3$-based compounds, including the $Ba(Zn_{1/3}Ta_{2/3})O_3$ (BZT), $Ba(Zn_{1/3}Ta_{1/3}Nb_{1/3})O_3$ (BZTN), $Ba(Zn_{1/6}Co_{1/6}Ta_{2/9}Nb_{2/9}Sb_{2/9})O_3$ (BZCTNS), and $Ba_{1/2}Sr_{1/2}(Zn_{1/6}Co_{1/6}Ta_{2/9}Nb_{2/9}Sb_{2/9})O_3$ (BSZCTNS) ceramics, sintered at different temperatures. For the $Ba(Zn_{1/3}Ta_{2/3})O_3$ ceramic, a maximum sintered density of 7.69 g/cm^3 (97.5% theoretical density) was reached at 1650 °C. With partial substitution of Ta^{5+} ions by Nb^{5+} ions, the $Ba(Zn_{1/}$

Table 1
Formulations of the $Ba(Zn_{1/3}Ta_{2/3})O_3$-based complex perovskites.

Formulation	Tolerance factor (t)	Spreading of t (Δt)	Composition (wt%)						
			$BaCO_3$	$SrCO_3$	ZnO	$CoCO_3$	Ta_2O_5	Nb_2O_5	Sb_2O_5
$Ba(Zn_{1/3}Ta_{2/3})O_3$	1.024	0.048	53.1	–	7.3	–	39.6	–	–
$Ba(Zn_{1/3}Ta_{1/3}Nb_{1/3})O_3$	1.024	0.048	57.7	–	7.9	–	21.5	12.9	–
$Ba(Zn_{1/6}Co_{1/6}Ta_{2/9}Nb_{2/9}Sb_{2/9})O_3$	1.027	0.072	57.1	–	3.9	5.7%	14.2	8.5	10.4
$Ba_{1/2}Sr_{1/2}(Zn_{1/6}Co_{1/6}Ta_{2/9}Nb_{2/9}Sb_{2/9})O_3$	0.999	0.128	30.8	23.1	4.2	6.2%	15.3	9.2	11.2

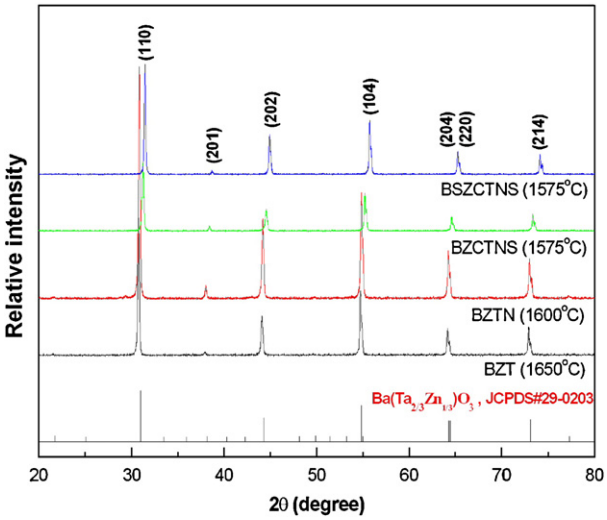

Fig. 2. XRD patterns of the $Ba(Zn_{1/3}Ta_{2/3})O_3$, $Ba(Zn_{1/3}Ta_{1/3}Nb_{1/3})O_3$, $Ba(Zn_{1/6}Co_{1/6}Ta_{2/9}Nb_{2/9}Sb_{2/9})O_3$, and $Ba_{1/2}Sr_{1/2}(Zn_{1/6}Co_{1/6}Ta_{2/9}Nb_{2/9}Sb_{2/9})O_3$ ceramics, at maximum densification.

$_3Ta_{1/3}Nb_{1/3})O_3$ ceramics reported a lower sintering temperature of 1600 °C. Similarly, both the $Ba(Zn_{1/6}Co_{1/6}Ta_{2/9}Nb_{2/9}Sb_{2/9})O_3$ and the $Ba_{1/2}Sr_{1/2}(Zn_{1/6}Co_{1/6}Ta_{2/9}Nb_{2/9}Sb_{2/9})O_3$ ceramics were observed to register lower densification temperatures of 1575 and 1550 °C, respectively. The sintering temperature of the $Ba(Zn_{1/3}Ta_{2/3})O_3$-based complex perovskite ceramics appeared to decrease as B-site or A-site ions were substituted by a multiplicity of ions.

Fig. 2 shows the XRD patterns of the $Ba(Zn_{1/3}Ta_{2/3})O_3$, $Ba(Zn_{1/3}Ta_{1/3}Nb_{1/3})O_3$, $Ba(Zn_{1/6}Co_{1/6}Ta_{2/9}Nb_{2/9}Sb_{2/9})O_3$, and $Ba_{1/2}Sr_{1/2}(Zn_{1/6}Co_{1/6}Ta_{2/9}Nb_{2/9}Sb_{2/9})O_3$ ceramics at maximum densification (sintered at the temperatures shown in Fig. 1). For $Ba(Zn_{1/3}Ta_{2/3})O_3$ sintered at 1650 °C, major peaks of (1 1 0), (2 0 1), (2 0 2), (1 0 4) (2 0 4), (2 2 0) and (2 1 4) were observed (indexed by JCPDS Card #29-0203). No other phase was detected based on the XRD results, and no indication of superlattice reflection was observed. With partial substitution of Ta^{5+} by Nb^{5+}, the XRD pattern of the $Ba(Zn_{1/3}Ta_{1/3}Nb_{1/3})O_3$ ceramic matched with that of the $Ba(Zn_{1/3}Ta_{2/3})O_3$ phase. Ta^{5+} and Nb^{5+} ions are identical in terms of ionic radius (0.64 Å) and electronic structure while Nb_2O_5 is isostructural with Ta_2O_5 [20,21]. Therefore, Nb_2O_5 is a logical substituent for Ta_2O_5 in complex perovskite compounds, and there was no visible shift on the XRD peaks. Further substitution of B-site by Co^{2+} and Sb^{5+} ions and A-site by Sr^{2+} ions of the complex perovskites, the $Ba(Zn_{1/6}Co_{1/6}Ta_{2/9}Nb_{2/9}Sb_{2/9})O_3$, and $Ba_{1/2}Sr_{1/2}(Zn_{1/6}Co_{1/6}Ta_{2/9}Nb_{2/9}Sb_{2/9})O_3$ ceramics were found to exhibit pure phases with XRD patterns similar to that of the $Ba(Zn_{1/3}Ta_{2/3})O_3$ ceramic. It appeared that the XRD peaks were moved to higher angles due to the fact that the ionic radii of Sr^{2+} (1.44 Å) and Sb^{5+} (0.60 Å) ions are smaller than those of Ba^{2+} (1.61 Å) and Ta^{5+} (0.64 Å) ions respectively [21]. Tolerance factors (t) of these compounds were calculated based on the following equation proposed by Reaney et al. [22]:

$$t = \frac{r_a + r_o}{\sqrt{2}(r_b + r_o)}$$

where t is the tolerance factor, r_a the average radius of the A site ions, r_b the average radius of the B site ions, and r_o the radius of the oxygen ions. As listed in Table 1, the calculated t-values of the $Ba(Zn_{1/3}Ta_{2/3})O_3$ based compounds range from 0.999 to 1.027. The t-values positioned within the limit of the stable perovskite formation [23,24] are in accord with the XRD results shown in Fig. 2. It is evident that variation in the t-value, instead of causing by the B-site substitution, was primarily controlled by the A-site occupancy, i.e., by the strontium content in the ceramics.

Fig. 3 shows the SEM images of the $Ba(Zn_{1/3}Ta_{2/3})O_3$, $Ba(Zn_{1/3}Ta_{1/3}Nb_{1/3})O_3$, $Ba(Zn_{1/6}Co_{1/6}Ta_{2/9}Nb_{2/9}Sb_{2/9})O_3$, and $Ba_{1/2}Sr_{1/2}(Zn_{1/6}Co_{1/6}Ta_{2/9}Nb_{2/9}Sb_{2/9})O_3$ ceramics, sintered at their individual maximum densification temperatures and subsequently annealed at 1400 °C for 24 h. Remarkable variations in the microstructure among these $Ba(Zn_{1/3}Ta_{2/3})O_3$ based compounds were observed, apparently due to the substantial differences in their composition. Similar to the results reported in the literature [11], the $Ba(Zn_{1/3}Ta_{2/3})O_3$ ceramic showed a microstructure composed of large grains in the sizes of 9–11 μm and scattering voids in the sizes of 2–4 μm [Fig. 3(a)]. The porous microstructure might be caused by the evaporation of ZnO during the sintering process. As revealed in Fig. 3(b), the $Ba(Zn_{1/3}Ta_{1/3}Nb_{1/3})O_3$ ceramic had a microstructure characterized by larger grains in the sizes of 20–40 μm and small pores. The grain growth mechanism, though unclear at present, may be associated with the formation of a liquid phase at high temperatures [8,11]. For the $Ba(Zn_{1/6}Co_{1/6}Ta_{2/9}Nb_{2/9}Sb_{2/9})O_3$ ceramic, the microstructure exhibited large grains 15–25 μm and voids 3–10 μm in size while the microstructure of the $Ba_{1/2}Sr_{1/2}(Zn_{1/6}Co_{1/6}Ta_{2/9}Nb_{2/9}Sb_{2/9})O_3$ ceramic appeared to be dense with small grains 3–5 μm in size. Fig. 3 apparently indicates that no second phase was formed during annealing, a finding further verified by the XRD results. Moreover, the changes in the grain size and grain size distribution are trivial, except for the differences in the porosity content.

Figs. 4–6 present respectively the dielectric constants (ε_r), quality factors ($Q \times f$), and temperature coefficients of resonance frequency (τ_f) for the $Ba(Zn_{1/3}Ta_{2/3})O_3$, $Ba(Zn_{1/3}Ta_{1/3}Nb_{1/3})O_3$, $Ba(Zn_{1/6}Co_{1/6}Ta_{2/9}Nb_{2/9}Sb_{2/9})O_3$, and $Ba_{1/2}Sr_{1/2}(Zn_{1/6}Co_{1/6}Ta_{2/9}Nb_{2/9}Sb_{2/9})O_3$ ceramics as a function of sintering temperature. As shown in Fig. 4, the dielectric constants of the $Ba(Zn_{1/3}Ta_{2/3})O_3$-based complex perovskites rise generally with the increasing sintering temperature. There is a good correlation between the growth in sintering density and the increase of dielectric constant. Porosity content in the ceramics seems to significantly dilute the magnitude of the dielectric constant value. The maximum dielectric constant of the dense $Ba(Zn_{1/3}Ta_{2/3})O_3$ ceramic sintered at 1650 °C appeared to be 29.8. With part of the Ta^{5+} ions substituted by Nb^{5+} ions, the dielectric constant of the $Ba(Zn_{1/3}Ta_{1/3}Nb_{1/3})O_3$ ceramic sintered at 1600 °C reached 34.2. With further replacement of the B-site ions by Co^{2+} and Sb^{5+} as well as A-site ions by Sr^{2+}, the $Ba(Zn_{1/6}Co_{1/6}Ta_{2/9}Nb_{2/9}Sb_{2/9})O_3$ ceramic sintered at 1575 °C and the $Ba_{1/2}Sr_{1/2}(Zn_{1/6}Co_{1/6}Ta_{2/9}Nb_{2/9}Sb_{2/9})O_3$ ceramic sintered at 1550 °C reported an obvious decline in

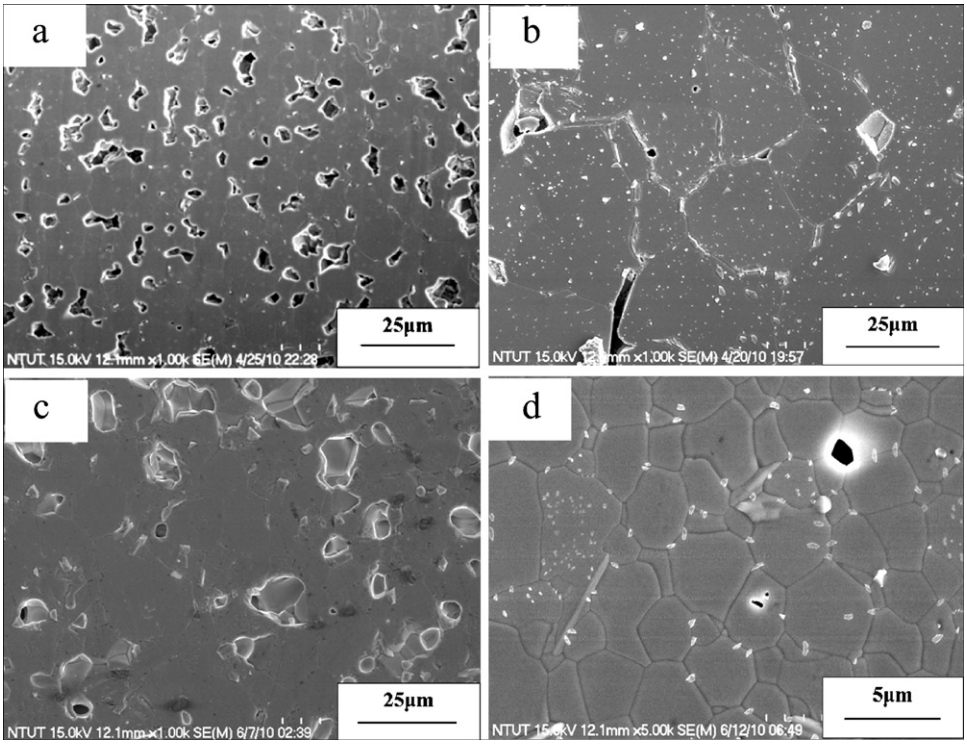

Fig. 3. SEM images of the (a) $Ba(Zn_{1/3}Ta_{2/3})O_3$ ceramic sintered at 1650 °C, (b) $Ba(Zn_{1/3}Ta_{1/3}Nb_{1/3})O_3$ ceramic sintered at 1600 °C, (c) $Ba(Zn_{1/6}Co_{1/6}Ta_{2/9}Nb_{2/9}Sb_{2/9})O_3$ ceramic sintered at 1575 °C, and (d) $Ba_{1/2}Sr_{1/2}(Zn_{1/6}Co_{1/6}Ta_{2/9}Nb_{2/9}Sb_{2/9})O_3$ ceramic sintered at 1500 °C, after annealing at 1400 °C for 24 h.

maximum dielectric constant that went down respectively to 24.9 and 26.3. The trends of the $Q \times f$ values with sintering temperature are also closely related to the variations in sintered density as shown in Fig. 1. It can be observed that the maximum $Q \times f$ value of 43,200 GHz for the as-sintered $Ba(Zn_{1/3}Ta_{2/3})O_3$ ceramic went up with the substitution of the B-site ions by Nb^{5+}, Co^{2+} and Sb^{5+} while the maximum $Q \times f$ values of the as-sintered $Ba(Zn_{1/3}Ta_{1/3}Nb_{1/3})O_3$ and $Ba(Zn_{1/6}Co_{1/6}Ta_{2/9}Nb_{2/9}Sb_{2/9})O_3$ ceramics read 52,500 and 68,000 GHz respectively. On the other hand, the $Q \times f$ value of the as-sintered $Ba_{1/2}Sr_{1/2}(Zn_{1/6}Co_{1/6}Ta_{2/9}Nb_{2/9}Sb_{2/9})O_3$ ceramic reached its maximum at 35,000 GHz. The $Q \times f$ value decreases significantly with Sr^{2+} substitution due to the formation of a less densely packed structure caused by the smaller ionic radius of the Sr^{2+} ion. With the increase in the Sr^{2+} content in the composition, the anharmonicity associated with the A-BO_6 vibration increases due to the growth in the amplitude of the vibration which in turn decreases the Q-factor [16]. In response to the rise in sintering temperature, τ_f went down slightly for the $Ba(Zn_{1/3}Ta_{2/3})O_3$ and $Ba_{1/2}Sr_{1/2}(Zn_{1/6}Co_{1/6}Ta_{2/9}Nb_{2/9}Sb_{2/9})O_3$ ceramics and moved

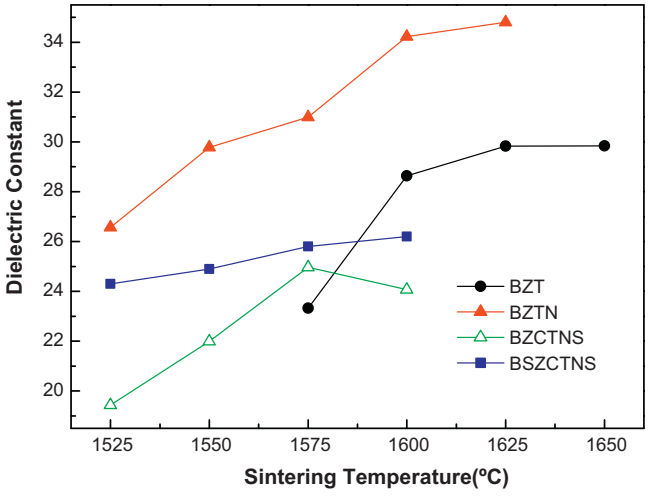

Fig. 4. Dielectric constants of the $Ba(Zn_{1/3}Ta_{2/3})O_3$, $Ba(Zn_{1/3}Ta_{1/3}Nb_{1/3})O_3$, $Ba(Zn_{1/6}Co_{1/6}Ta_{2/9}Nb_{2/9}Sb_{2/9})O_3$, and $Ba_{1/2}Sr_{1/2}(Zn_{1/6}Co_{1/6}Ta_{2/9}Nb_{2/9}Sb_{2/9})O_3$ ceramics as a function of sintering temperature.

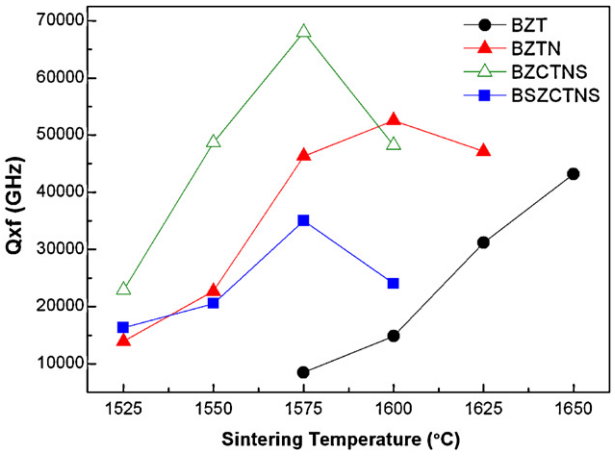

Fig. 5. Quality factors of the $Ba(Zn_{1/3}Ta_{2/3})O_3$, $Ba(Zn_{1/3}Ta_{1/3}Nb_{1/3})O_3$, $Ba(Zn_{1/6}Co_{1/6}Ta_{2/9}Nb_{2/9}Sb_{2/9})O_3$, and $Ba_{1/2}Sr_{1/2}(Zn_{1/6}Co_{1/6}Ta_{2/9}Nb_{2/9}Sb_{2/9})O_3$ ceramics as a function of sintering temperature.

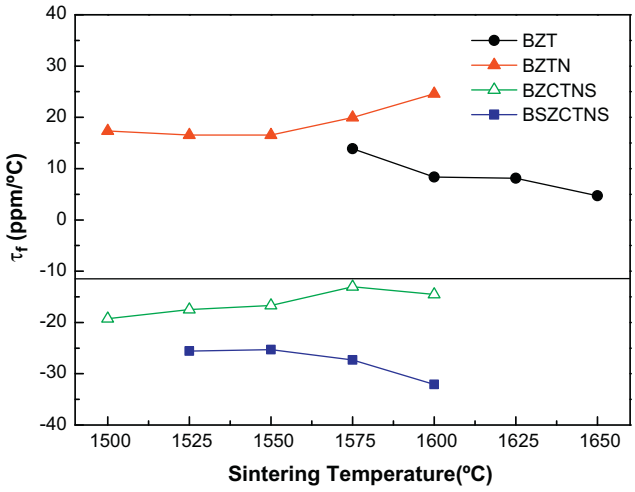

Fig. 6. Temperature coefficients of resonance frequency (τ_f) of the $Ba(Zn_{1/3}Ta_{2/3})O_3$, $Ba(Zn_{1/3}Ta_{1/3}Nb_{1/3})O_3$, $Ba(Zn_{1/6}Co_{1/6}Ta_{2/9}Nb_{2/9}Sb_{2/9})O_3$, and $Ba_{1/2}Sr_{1/2}(Zn_{1/6}Co_{1/6}Ta_{2/9}Nb_{2/9}Sb_{2/9})O_3$ ceramics as a function of sintering temperature.

up a little for the $Ba(Zn_{1/3}Ta_{1/3}Nb_{1/3})O_3$ and $Ba(Zn_{1/6}Co_{1/6}Ta_{2/9}Nb_{2/9}Sb_{2/9})O_3$, ceramics. The τ_f values of the $Ba(Zn_{1/3}Ta_{2/3})O_3$, $Ba(Zn_{1/3}Ta_{1/3}Nb_{1/3})O_3$, $Ba(Zn_{1/6}Co_{1/6}Ta_{2/9}Nb_{2/9}Sb_{2/9})O_3$, and $Ba_{1/2}Sr_{1/2}(Zn_{1/6}Co_{1/6}Ta_{2/9}Nb_{2/9}Sb_{2/9})O_3$ ceramics with maximum quality factors read respectively 4.71, 19.97, −13.05, and −25.3 ppm/°C. The τ_f value is correlated to the τ_ε value through the following formula and thus tied with the tolerance factor "t".

$$\tau_f = -\left(\frac{1}{2}\tau_\varepsilon + \alpha_L\right)$$

where τ_ε is the temperature coefficient of the dielectric constant and α_L the linear expansion coefficient. A comparison of the τ_f values and the tolerance factors listed in Table 1 finds the data in fair agreement with the pattern of Reaney's results, except for that of the $Ba(Zn_{1/6}Co_{1/6}Ta_{2/9}Nb_{2/9}Sb_{2/9})O_3$ ceramic.

The $Ba(Zn_{1/3}Ta_{2/3})O_3$-based complex perovskites with peak microwave dielectric properties were further subjected to annealing at 1400 °C for 10 and 24 h. The annealed samples were then characterized with the results summarized in Table 2. The post-annealing appeared to have little effect on ε_r and τ_f values of the $Ba(Zn_{1/3}Ta_{2/3})O_3$-based complex perovskite, while a remarkable change occurred in the $Q \times f$ values, a finding echoing the one reported in the literature [17]. The $Q \times f$ value of the $Ba(Zn_{1/3}Ta_{2/3})O_3$ ceramic escalated dramatically from 43,200 to 121,600 GHz after annealing at 1400 °C for 10 h but started to drop as the annealing continued up to 24 h, probably due to ZnO evaporation. For the $Ba(Zn_{1/3}Ta_{1/3}Nb_{1/3})O_3$ ceramic, the $Q \times f$ values read 53,160 GHz and 104,100 GHz after annealed at 1400 °C for 10 h and 24 h respectively. Similar to the trend for the $Ba(Zn_{1/3}Ta_{2/3})O_3$ ceramic, the $Ba(Zn_{1/6}Co_{1/6}Ta_{2/9}Nb_{2/9}Sb_{2/9})O_3$ ceramic witnessed its $Q \times f$ value rise to 83,000 GHz after annealing at 1400 °C for 10 h and then plunge to 46,000 GHz as the annealing went on to 24 h. The $Ba_{1/2}Sr_{1/2}(Zn_{1/6}Co_{1/6}Ta_{2/9}Nb_{2/9}Sb_{2/9})O_3$ ceramic nevertheless revealed no significant variation in $Q \times f$ value after annealing. Generally speaking, $Q \times f$ value is expected to decrease dramatically with the growth in the types of ions substituting the B-site and A-site ions due to the increase in entropy. This accordingly may lessen the ion ordering. However, it is worth noting that, while the $Q \times f$ value did undergo decline in this study, the magnitude of the decline was not as significant as expected. One possible explanation for the high $Q \times f$ values of the $Ba(Zn_{1/3}Ta_{2/3})O_3$, $Ba(Zn_{1/3}Ta_{1/3}Nb_{1/3})O_3$, and $Ba(Zn_{1/6}Co_{1/6}Ta_{2/9}Nb_{2/9}Sb_{2/9})O_3$ ceramics and the low $Q \times f$ value of the $Ba_{1/2}Sr_{1/2}(Zn_{1/6}Co_{1/6}Ta_{2/9}Nb_{2/9}Sb_{2/9})O_3$ ceramic is the difference in the spreading of ionic radius on the A-site and B-site, i.e., the spreading of tolerance factor (Δt) as proposed by Reaney and Iddles [23]. For instance, the Δt for the $Ba(Zn_{1/6}Co_{1/6}Ta_{2/9}Nb_{2/9}Sb_{2/9})O_3$ ceramic can be calculated using the t-values calculated from the combinations as follows: Ba^{2+} and Zn^{2+}, Ba^{2+} and Co^{2+}, Ba^{2+} and Ta^{5+}, Ba^{2+} and Nb^{5+}, and Ba^{2+} and Sb^{5+}. The t for each of these combinations is calculated, and the largest and smallest values are taken to give Δt. As shown in Table 1, the $Ba_{1/2}Sr_{1/2}(Zn_{1/6}Co_{1/6}Ta_{2/9}Nb_{2/9}Sb_{2/9})O_3$ ceramic reports the largest Δt calculated, representing a large range of bond lengths on the A and B sites which would result in greater anharmonicity and dampening of phonon modes, thereby decreasing the $Q \times f$ value.

Table 2
Microwave dielectric properties of the $Ba(Zn_{1/3}Ta_{2/3})O_3$-based complex perovskites.

Formulation	Sintering condition	Annealing condition	Bulk density (g/cm^3)	ε_r	f_0 (GHz)	$Q \times f$ (GHz)	τ_f (ppm/°C)
$Ba(Zn_{1/3}Ta_{2/3})O_3$	1650 °C/6 h	–	7.69	29.8	10.03	43,200	4.71
		1400 °C/10 h	7.74	28.2	10.07	121,600	5.31
		1400 °C/24 h	7.79	26.9	10.40	113,700	6.27
$Ba(Zn_{1/3}Ta_{1/3}Nb_{1/3})O_3$	1600 °C/6 h	–	6.96	34.2	8.86	52,560	19.97
		1400 °C/10 h	7.08	34.4	8.85	53,160	18.26
		1400 °C/24 h	7.04	33.4	8.92	104,000	17.96
$Ba(Zn_{1/6}Co_{1/6}Ta_{2/9}Nb_{2/9}Sb_{2/9})O_3$	1575 °C/6 h	–	6.57	24.9	10.34	68,000	−13.05
		1400 °C/10 h	6.52	24.9	10.35	83,000	−12.68
		1400 °C/24 h	6.33	24.8	10.34	46,000	−13.54
$Ba_{1/2}Sr_{1/2}(Zn_{1/6}Co_{1/6}Ta_{2/9}Nb_{2/9}Sb_{2/9})O_3$	1550 °C/6 h	–	6.89	26.3	9.85	35,000	−25.3
		1400 °C/10 h	7.08	27.0	9.32	32,100	−22.6
		1400 °C/24 h	6.97	28.6	8.87	35,700	−22.9

4. Summary

Complex perovskite compounds of $Ba(Zn_{1/3}Ta_{2/3})O_3$, $Ba(Zn_{1/3}Ta_{1/3}Nb_{1/3})O_3$, $Ba(Zn_{1/6}Co_{1/6}Ta_{2/9}Nb_{2/9}Sb_{2/9})O_3$, $Ba_{1/2}Sr_{1/2}(Zn_{1/6}Co_{1/6}Ta_{2/9}Nb_{2/9}Sb_{2/9})O_3$ ceramics were prepared and characterized in this study. The sintering temperatures of these compounds ranged from 1550 to 1650 °C. The XRD patterns showed no formation of second phase. After post-annealing, most of the $Q \times f$ values were observed to sustain improvement. The $Ba(Zn_{1/6}Co_{1/6}Ta_{2/9}Nb_{2/9}Sb_{2/9})O_3$ ceramic sintered at 1575 °C for 6 h and followed by annealing at 1400 °C for 10 h reported an ε_r of 24.9, a $Q \times f$ value of 83,000 GHz, and a τ_f of −12.8 ppm/°C, while the $Ba_{1/2}Sr_{1/2}(Zn_{1/6}Co_{1/6}Ta_{2/9}Nb_{2/9}Sb_{2/9})O_3$ ceramic, sintered at 1550 °C for 6 h and annealed at 1400 °C for 10 h, registered an ε_r of 27.0, a $Q \times f$ value of 32,100 GHz, and a τ_f of −22.6 ppm/°C.

References

[1] H.M. O'Bryan Jr., J.K. Plourde, J. Thomson Jr., Dielectric for microwave application, US Patent 4,563,661 (1986).

[2] D. Kolar, Z. Stadler, S. Gaberscek, D. Suvorov, Ceramic and dielectric properties of selected compositions in the $BaO–TiO_2–Nd_2O_3$ system, Ber. Dr. Keram. Ges. 55 (1978) 346–347.

[3] D. Kolar, S. Gaberscek, B. Volavsek, Synthesis and crystal chemistry of $BaNdTi_3O_{10}$, $BaNd_2Ti_5O_{14}$, and $Nd_4Ti_5O_{24}$, J. Solid State Chem. 38 (1981) 58–164.

[4] H. Ohsato, Science of tungstenbronze-type like $Ba_{6-3x}R_{8+2x}Ti_{18}O_{54}$ (R = rare earth) microwave dielectric solid solutions, J. Eur. Ceram. Soc. 21 (2001) 2701–2711.

[5] R. Freer, F. Azouh, Microstructural engineering of microwave dielectric ceramics, J. Eur. Ceram. Soc. 28 (2008) 1433–1441.

[6] S. Kawashima, M. Nishida, I. Ueda, H. Ouchi, $Ba(Zn_{1/3}Ta_{2/3})O_3$ ceramics with low dielectric loss at microwave frequencies, J. Am. Ceram. Soc. 66 (6) (1983) 421–423.

[7] S.J. Webb, J. Breeze, R.I. Scott, D.S. Cannell, D.M. Iddles, N.M. Alford, Raman spectroscopic study of gallium-doped $Ba(Zn_{1/3}Ta_{2/3})O_3$, J. Am. Ceram. Soc. 85 (7) (2002) 1753–1756.

[8] I. Qazi, I.M. Reaney, W.E. Lee, Order-disorder phase transition in $Ba(Zn_{1/3}Ta_{2/3})O_3$, J. Eur. Ceram. Soc. 21 (2001) 2613–2616.

[9] C.C. Lee, C.C. Chou, D.S. Tsai, Effect of La/K A-site substitutions on the ordering of $Ba(Zn_{1/3}Ta_{2/3})O_3$, J. Am. Ceram. Soc. 80 (11) (1997) 2885–2890.

[10] D.J. Barber, K.M. Moulding, J.I. Zhou, Structural order in $Ba(Zn_{1/3}Ta_{2/3})O_3$, $Ba(Zn_{1/3}Nb_{2/3})O_3$ and $Ba(Mg_{1/3}Ta_{2/3})O_3$ microwave dielectric ceramics, J. Mater. Sci. 32 (1997) 1531–1544.

[11] C.J. Lee, G. Pezzotti, S.H. Kang, D.J. Kim, K.S. Hong, Quantitative analysis of lattice distortion in $Ba(Zn_{1/3}Ta_{2/3})O_3$ microwave ceramics with added B_2O_3 using Raman spectroscopy, J. Eur. Ceram. Soc. 26 (2006) 1385–1391.

[12] H. Tamura, D.A. Sagaia, K. Wakino, Lattice vibrations of $Ba(Zn_{1/3}Ta_{2/3})O_3$ crystal with ordered perovskite structure, Jpn. J. Appl. Phys. 25 (6) (1986) 787–791.

[13] S.B. Desu, H.M. O'Bryan, Microwave loss quality of $Ba(Zn_{1/3}Ta_{2/3})O_3$ ceramics, J. Am. Ceram. Soc. 68 (1985) 546–551.

[14] H. Tamura, T. Konoike, Y. Sakabe, K. Wakino, Improved high Q dielectric resonator with complex perovskite structure, J. Am. Ceram. Soc. 67 (1984) C59–C61.

[15] P.K. Davies, J.U. Tong, Effect of ordering-induced domain boundaries on low-loss $Ba(Zn_{1/3}Ta_{2/3})O_3–BaZrO_3$ perovskite microwave dielectrics, J. Am. Ceram. Soc. 80 (7) (1997) 1727–1740.

[16] J. Venkatesh, V.S.K. Murthy, Microwave dielectric properties of $(Ba,Sr)(Zn_{1/3}Ta_{2/3})O_3$ dielectric resonators, Mater. Chem. Phys. 58 (1999) 276–279.

[17] K. Kageyama, Crystal structure and microwave dielectric properties of $Ba(Zn_{1/3}Ta_{2/3})O_3–(Sr,Ba)(Ga_{1/2}Ta_{1/2})O_3$ ceramics, J. Am. Ceram. Soc. 75 (7) (1992) 1767–1771.

[18] M.K. Lee, J.H. Chung, K.W. Ryu, Y.H. Lee, Microwave dielectric properties of $Ba(Mg,Ta)O_3–Ba(Co,Nb)O_3$ ceramics, in: Proceedings of 1998 International Symposium on Electrical Insulating Materials, in Conjunction with 1998 Asian International Conference on Dielectrics and Electrical Insulation and the 30th Symposium on Electrical Insulating Materials, Toyohashi, Japan, September 27–30, 1998.

[19] B.W. Hakki, P.D. Coleman, A dielectric resonator method of measuring inductive in the millimeter range, IRE Trans. Microwave Theory Tech. MTT-8 (1960) 402–410.

[20] I.M. Reaney, Y. Iqbal, H. Zheng, A. Feteira, H. Hughes, D. Iddles, D. Muir, T. Prices, Order-disorder behavior in $0.9([Zn_{0.60}Co_{0.40}]_{1/3}Nb_{2/3})O_3–0.1Ba(Ga_{0.5}Ta_{0.5})O_3$ microwave dielectric resonators, J. Eur. Ceram. Soc. 25 (2005) 1183–1189.

[21] R.D. Shannon, Revised effective ionic radii and systematic studies of interatomic distances in halides and chalcogenides, Acta Crystallogr. A 32 (1976) 751–767.

[22] I.M. Reaney, E.L. Colla, N. Setter, Dielectric and structural characteristics of Ba- and Sr-based complex perovskites as a function of tolerance factor, Jpn. J. Appl. Phys. 33 (1994) 3984–3990.

[23] I.M. Reaney, D. Iddles, Microwave dielectric ceramics for resonators and filters in mobile phone networks, J. Am. Ceram. Soc. 89 (2006) 2063–2072.

[24] C.J. Hampson, R.I. Scott, C.N. Elgy, M.G. Thomas, Permittivity and temperature response of complex niobate perovskite dielectrics, J. Eur. Ceram. Soc. 24 (2004) 3739–3745.